Strong-field control of the dissociative ionization of N$_2$O with near-single-cycle pulses

M Kübel[1,2], **A S Alnaser**[2,3,4], **B Bergues**[2], **T Pischke**[2], **J Schmidt**[1], **Y Deng**[2],
C Jendrzejewski[1], **J Ullrich**[5,6], **G G Paulus**[7,8], **A M Azzeer**[4], **U Kleineberg**[1],
R Moshammer[5] **and M F Kling**[1,2]

[1] Ludwig-Maximilians-Universität München, D-85748 Garching, Germany
[2] Max-Planck-Institut für Quantenoptik, D-85748 Garching, Germany
[3] Physics Department, American University of Sharjah, POB26666, Sharjah, UAE
[4] Department of Physics & Astronomy, King-Saud University, Riyadh 11451, Saudi Arabia
[5] Max-Planck-Institut für Kernphysik, D-69117 Heidelberg, Germany
[6] Physikalisch-Technische Bundesanstalt, D-38116 Braunschweig, Germany
[7] Institut für Optik und Quantenelektronik, D-07743 Jena, Germany
[8] Helmholtz Institut Jena, D-07743 Jena, Germany
E-mail: matthias.kuebel@mpq.mpg.de

Abstract

The dissociative ionization of N$_2$O by near-single-cycle laser pulses is studied using phase-tagged ion–ion coincidence momentum imaging. Carrier–envelope phase (CEP) dependences are observed in the absolute ion yields and the emission direction of nearly all ionization and dissociation pathways of the triatomic molecule. We find that laser-field-driven electron recollision has a significant impact on the dissociative ionization dynamics and results in pronounced CEP modulations in the dication yields, which are observed in the product ion yields after dissociation. The results indicate that the directional emission of coincident N$^+$ and NO$^+$ ions in the denitrogenation of the dication can be explained by selective ionization of oriented molecules. The deoxygenation of the dication with the formation of coincident N$_2^+$ + O$^+$ ions exhibits an additional shift in its CEP dependence, suggesting that this channel is further influenced by laser interaction with the dissociating dication. The experimental

results demonstrate how few-femtosecond dynamics can drive and steer molecular reactions taking place on (much) longer time scales.

1. Introduction

The interplay between electronic and nuclear motion is at the heart of chemical reactions. Recent progress in controlling (coupled) ultrafast electronic and nuclear motion was fueled by the development of intense ultrashort light pulses with controlled waveform [1–4]. The waveform of such pulses can be used as a reagent to coherently control molecular dynamics [5] and charge-directed reactivity [6, 7]. A suitable parameter for modifying the electric field waveform of a few-cycle pulse, $E(t) = E_0(t)\cos(\omega t + \phi)$, with envelope $E_0(t)$, and carrier frequency ω, is the carrier–envelope phase (CEP) ϕ. The CEP control of molecular dynamics has been predominantly investigated for diatomic molecules in both experiment and theory [5, 8]. A large part of previous work was performed on molecular hydrogen and molecular hydrogen ions (see e.g. [7, 9–27]). These studies have established that the control may involve the following CEP-dependent processes: (1) the laser ionization and excitation of the molecule, (2) field-driven electron recollision dynamics leading to further ionization and excitation, and (3) the laser dressing and laser-induced coupling of states. The strongly driven, coupled (and correlated) electron–nuclear dynamics typically needs to be described by models beyond the Born–Oppenheimer approximation (see e.g. [5]). Light pulses in the extreme ultraviolet, used in pump–probe schemes, in combination with such intense few-cycle pulses, enable the tracing of the molecular dynamics with time resolutions reaching into the attosecond regime for hydrogen [28–30] and other molecules [31–36].

Despite the wealth of studies on the sub-cycle control of the ionization and dissociation of diatomic systems, work on systems beyond molecular hydrogen is less abundant. Experimental examples for diatomics include the sub-cycle control of the ionization and dissociative ionization of O_2 [34], N_2 [37], CO [20, 38–40], DCl [41], and K_2 [42]. Data for larger and more complex molecules are scarce. Recently, Xie *et al* investigated the CEP control of the yields of the dissociative ionization and isomerization of hydrocarbons [43]. They found that laser-driven recollisional ionization and excitation caused a π-periodic oscillation of the ionization and fragmentation yields with CEP. Mathur *et al* studied the strong-field dissociative ionization dynamics of CS_2 molecules and found CEP-dependent modulations in the fragmentation yields [44]. Processes depending on the direction of the electric field have also been predicted for larger molecules (see e.g. [45–47]), and, only recently, evidence for the control of the preferential direction of proton ejection from hydrocarbons has been reported [48, 49].

Here, we extend the studies on complex systems and investigate the CEP dependence of the dissociative ionization of N_2O molecules in strong, near-single-cycle laser fields. Employing coincident three-dimensional momentum imaging, we analyze the CEP control of the yields and also the directionality of the emission of dissociation fragments for two competing reaction channels. N_2O is a linear, asymmetric molecule with an N–N bond length of 1.13 Å and an N–O bond length of 1.19 Å. The relevant potentials for the dissociation of N_2O^{2+} are displayed in
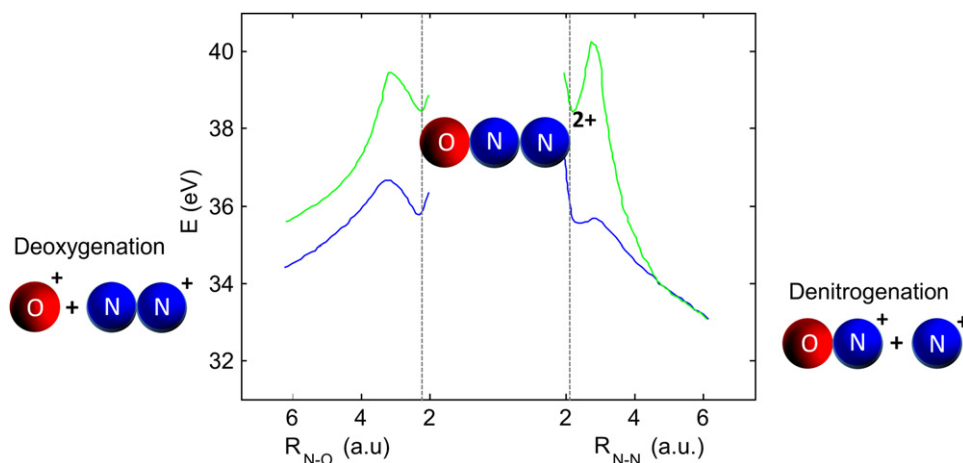
Figure 1. Potential energy curves for the two stretching coordinates in the two lowest electronic states of N_2O^{2+}, $3\Sigma^-$ (blue) and 3Π (green). The other stretching coordinate is at the corresponding equilibrium distance of the other bond, of $R_{N-N}^0 = 2.09$ a.u. and $R_{N-O}^0 = 2.22$ a.u., respectively, indicated by the dashed line. The lowest dissociation limits are 28.8 eV for denitrogenation and 30.9 eV for deoxygenation. The dissociation limit for the N–O stretching coordinate of the 3Π state is 32.4 eV. Adapted from [50].

figure 1. The direct single-ionization and double-ionization potentials of N_2O are 12.9 eV and 35.5 eV, respectively. Double ionization of N_2O below the threshold can occur via autoionizing states of N_2O^+ [51]. The enhancement of the double ionization of N_2O after the formation of highly excited, autoionizing states of the cation by an extreme ultraviolet pulse through a time-delayed infrared pulse was investigated by Zhou *et al* [33]. They found that the highly excited, inner–valence ionized N_2O^{+*} molecular ions decay rapidly through autoionization or dissociation in about 20 fs. Recently, Kotsina *et al* studied the generation of N^+ and NO^+ from N_2O induced by two-color (800 nm + 400 nm) 40 fs laser fields [52] and observed pronounced dependences of the yields and direction of the ion emission on the relative phase of the two colors. In particular, they interpreted the phase dependence of the left/right yields of N^+ and NO^+ along the linear polarization axis of the laser as a signature of the contribution of two channels. The two-color control scheme that was introduced as phase control by Brumer and Shapiro [53–56] is related to the present CEP control studies. In both approaches the electric field waveform can be tailored on a sub-cycle time scale [57]. The near-single-cycle pulses used in our study, however, provide additional insight into the field-driven N^+ formation. First, the short pulse duration permits limiting recollisional excitation and ionization to a single event [58], avoiding the complex excitation and ionization dynamics resulting from multiple recollisions in longer pulses. Second, the pulse duration is relatively short as compared to the nuclear dynamics, and some processes, such as charge resonance enhanced ionization occurring at large internuclear distances, are significantly reduced or completely avoided [11, 27]. Furthermore, we directly compare the dynamics of N^+ formation to that of the competing O^+ channel, taking advantage of our coincident detection scheme.

2. Experimental details

The experimental setup has been outlined previously [59]. Briefly, 4 fs laser pulses with a central wavelength of 750 nm are generated in a few-cycle laser system at a repetition rate of 10 kHz. A fraction of the laser beam (approximately 20 μJ) is focused into a single-shot Stereo-ATI phase meter [60, 61] to measure the CEP of every single laser shot. The remaining part of the beam passes through ultra-broadband quarter-wave and half-wave plates before being focused into a gas jet in the center of a reaction microscope [62] (REMI). The quarter-wave and half-wave plates can be used to adjust the polarization of the laser. Individual pairs of fused silica wedges are used in each arm of the beam path to ensure near-Fourier-limited pulses in both instruments. Ions generated in the laser focus in the REMI are directed towards a time-sensitive and position (x/y)-sensitive detector by a homogeneous electric field of approximately 60 V m^{-1}. The molecules in the gas jet travel along the y-axis while the laser propagates along the x-axis. For linearly polarized pulses, the electric field is polarized in the direction of the z-axis which coincides with the time-of-flight (TOF) direction of the ion spectrometer. The count rate was of the order of one event per laser shot, which permitted the analysis of ion–ion coincidences.

All possible singly charged ions from the dissociation of N_2O, namely N^+, O^+, N_2^+ and NO^+, were detected in our experiment. However, the TOF ranges of the different ion species overlap due to their large momenta acquired in the dissociation process. Thus, momentum spectra for non-coincident ions can only be generated by selection of one half of the full momentum distributions along the TOF axis and subsequent symmetrization. The situation is different for coincident ion detection, where the REMI provides the full momentum distribution for a momentum matched pair of ionic fragments.

Notably, no stable N_2O^{2+} ions were detected in the experiment, implying that the formation of the dication necessarily leads to dissociation. However, the tail observed in the photoion–photoion coincidence (PIPICO) spectrum for N^+ formation (see figure 2) indicates that a fraction of the dications dissociate via metastable states. These states decay as the dication goes towards the detector, resulting in a shift of the TOFs of N^+ and NO^+ towards the TOF value of 3.32 μs expected for the dication. Since no noteworthy yield of N_2O^{2+} was detected, the lifetime of the metastable states can be estimated from the length of the tail as a few 100 ns, in agreement with earlier experimental results [63]. The small fraction of ions decaying via metastable states have not been considered in our analysis of the ion momenta. Notably, the deoxygenation does not exhibit such a tail, indicating that the relevant excited states decay much more quickly.

The N_2O^{2+} recoil momenta prior to dissociation may still be obtained. For this purpose, we can take the momentum sum of the two coincident fragmentation channels:

(i) *denitrogenation*, $N_2O^{2+} \rightarrow N^+ + NO^+$, and

(ii) *deoxygenation*, $N_2O^{2+} \rightarrow O^+ + N_2^+$.

Using momentum conservation as a filter, the coincident events can be identified with very low uncertainty, despite the considerable number of non-coincident ions (see figure 2).
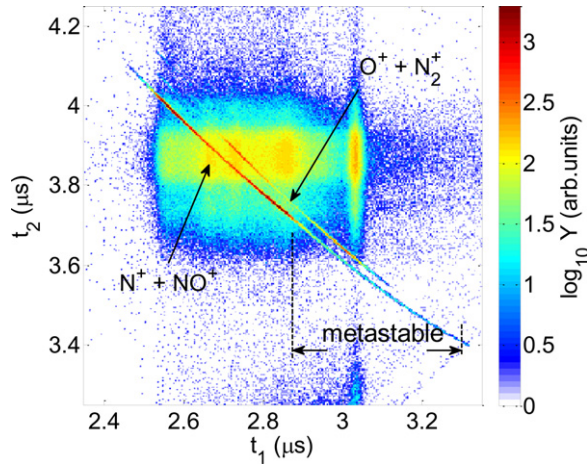
Figure 2. The relevant section of the PIPICO spectrum that permits the identification of coincident fragmentation channels. The ion yield Y is plotted on a logarithmic scale as a function of the TOFs of the ions detected first and second. The sharp lines are a consequence of the momentum conservation during the dissociation of the molecular ion and can be assigned to two dissociation channels, as indicated. The arrows point to the TOFs corresponding to zero momentum along the spectrometer axis for each ion (N^+/NO^+ and O^+/N_2^+, respectively). Traces of dissociation into N^+ and NO^+ via metastable states are also marked.

3. Single and double ionization of N₂O

Calculating the vector momentum sum of two coincident fragments yields the recoil momentum of the doubly charged ion just after the ionization by the laser pulse, and before the subsequent dissociation. This permits us to distinguish the momenta acquired during ionization and dissociation and investigate their CEP dependence separately. We will make use of this capability when comparing asymmetries in the fragment momenta to the ones in the cation and dication recoil momenta. Figure 3(a) shows that the momentum distribution of the N_2O^{2+} ions, prior to denitrogenation, exhibits a very strong CEP-dependent oscillation. Comparison of this result to the non-sequential double ionization (NSDI) of Ar^{2+} [58, 59] and N_2^{2+} [37] suggests that for the given laser conditions, the double ionization of N₂O is mainly induced by laser-driven electron recollision. For a more quantitative analysis, an asymmetry parameter is introduced as

$$A\left(\phi\right) = \frac{N_+\left(\phi\right) - N_-\left(\phi\right)}{N_+\left(\phi\right) + N_-\left(\phi\right)}, \tag{1}$$

where $N_{+/-}$ are the numbers of detected ions with positive/negative momenta along the laser polarization direction. Usually, the asymmetry can be parameterized as a sinusoidal $A\left(\phi\right) = A_0 \sin\left(\phi + \phi_0\right)$, where A_0 is the asymmetry amplitude, and ϕ_0 denotes a phase offset. As shown in figure 3(b), the asymmetries for the singly (crosses) and doubly charged (open circles) N₂O ions exhibit a phase shift of 120° with respect to each other. It may be tempting to directly interpret the CE phase shift as a time delay. The origin of the phase difference in the ion emission asymmetry, however, is more complex and requires the modeling of the double-
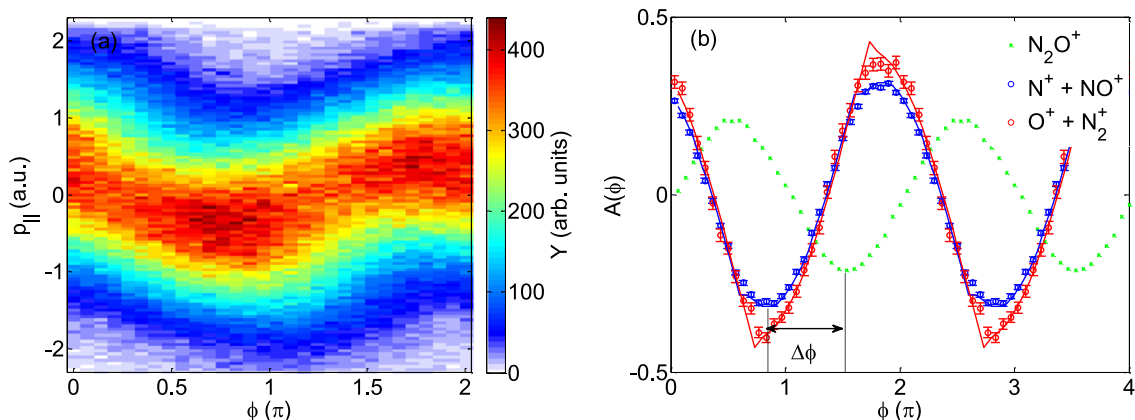
Figure 3. (a) CEP-resolved momentum spectrum along the laser polarization direction for N_2O^{2+}, obtained from the momentum sum of coincident N^+ and NO^+ fragments (note that the spectrum derived from the deoxygenation channel looks almost identical). (b) Asymmetries A in the recoil ion yields along the laser polarization direction for singly (green crosses) and doubly charged (open circles) N_2O ions. The latter are retrieved from the coincidences for the two dissociation pathways, denitrogenation (blue open circles) and deoxygenation (red open circles). They represent the asymmetries in the dication recoil momenta prior to dissociation into either of the two channels. The solid lines display predictions from a semi-classical model (see the text). The phase shift $\Delta\phi = 120°$ between the asymmetry curves for single and double ionization is indicated.

ionization process. In the absence of such calculations for N_2O, qualitative insight can be gained by comparison to the NSDI of Ar [58] and N_2 [37], where a phase shift of $120°$ between single and double ionization was found to be consistent with double ionization via electron recollision. The strong 20% asymmetry measured for N_2O^+ is a consequence of the very short pulse duration. Its offset ϕ_0 is employed as a universal reference for CEP offsets throughout this paper.

It is known that recollision-induced dynamics can be strongly suppressed with circularly polarized pulses. When the laser polarization is changed from linear to circular in our experiment, the asymmetry amplitude for the dication decreases to about the value for the cation, and the phase shift between singly and doubly charged ions reduces to only $10°$. Both an almost identical amplitude and a minimal phase shift corroborate the assertion that the ionization is predominantly laser driven and, in contrast to the situation with linear polarization, recollision is negligible.

Interestingly, with linear polarization the asymmetries in the momentum sums of the two dissociation pathways, deoxygenation and denitrogenation, have slightly different amplitudes. Figure 3(b) shows that the preparation of the dication undergoing deoxygenation is more sensitive to the CEP as compared to the dication preparation before denitrogenation. It is known from theory (see e.g. figure 1) and experiment (see e.g. [64]) that deoxygenation requires a few eV of extra energy as compared to denitrogenation. Having established that the dication is formed via electron recollision for both dissociation channels, the differences for the CEP dependence of the formation of the dication prior to denitrogenation and deoxygenation can likely be explained by the CEP dependence of the recolliding electron energy. In order to test this hypothesis we have performed a semi-classical simulation in which we use the ionization

rate given in [65] to calculate the CEP-dependent spectra of recolliding electrons ionized from an artificial atom of the same ionization potential as N_2O by a 4 fs laser pulse. Two different asymmetry curves are obtained by analyzing the calculated left–right yields above some energy values E_1 and E_2. We chose $E_1 = 22.5\,\text{eV}$ and $E_2 = 25\,\text{eV}$, corresponding to the direct ionization potential of N_2O^+ and an extra 3 eV to initiate deoxygenation, respectively. The resulting curves are found to closely mimic the measured asymmetries in the dication momenta prior to dissociation. The amplitudes of these calculated asymmetries depend on the intensity and pulse duration used for the simulation. They closely match the measurement for an instantaneous peak intensity of $I = 3.0 \times 10^{14}\,\text{W cm}^{-2}$ and a pulse duration $\tau = 4.1$ fs; see 3(b). Hence, the assumption that the stronger CEP dependence in the preparation of the deoxygenation is caused by the additional recollision energy required to populate the relevant states appears reasonable.

4. Analysis of non-coincident fragments

We now analyze the kinetic energy spectra and CEP dependences of the N^+, NO^+, O^+ and N_2^+ fragments without coincidence filtering. The corresponding energy spectra and asymmetry maps are shown in figure 4. Low-energy (below 1 eV) and high-energy channels can be distinguished for each of the four singly charged fragments. The high-energy channels are also present with coincidence filtering and include the deoxygenation and denitrogenation pathways, but are not necessarily restricted to these. In the case of O^+ and especially for N_2^+, a significant number of non-coincidence ions are present in the high-energy range. The coincidences will be discussed in detail in section 5. The low-energy ranges are only observed for non-coincident ions. Their energies and high yields suggest that they originate from the dissociation of the N_2O cation into the detected ion and a neutral fragment.

For each fragment, CEP-dependent asymmetries in the preferential emission direction along the laser polarization axis are observed in the low- and high-energy regions. The amplitudes A_0 and phase offsets ϕ_0 of the CEP-dependent asymmetries for all channels are summarized in table 1. Evidently, the high-energy channels exhibit a stronger CEP dependence than the low-energy ones, similar to the case for the observed amplitudes of the asymmetries for the creation of the N_2O cation and dication; see figure 3.

A full interpretation of the CEP effects would require the theoretical modeling of the data, which is challenging. To the best of our knowledge, CEP effects for the dissociation of even diatomic molecules from different charge states have not been quantitatively modeled. Our data might provide further motivation for developing such models. Here, we attempt to interpret the results on their own basis and via comparison to similar results for other molecules.

In order to gain more insight into our experimental observations, we first consider the CEP offsets of the low-energy channels. The asymmetries for N^+/N_2^+ fragments on one hand and O^+/NO^+ fragments on the other hand oscillate in phase and are shifted by approximately 180° with respect to each other. The comparison to the asymmetry in the N_2O^+ recoil momentum shows that N^+/N_2^+ emissions follow the preferential direction of motion of the cation, whereas for O^+/NO^+ the emission is in the opposite direction. The fact that the ion asymmetries are either in phase or shifted by 180° with respect to the cation asymmetry
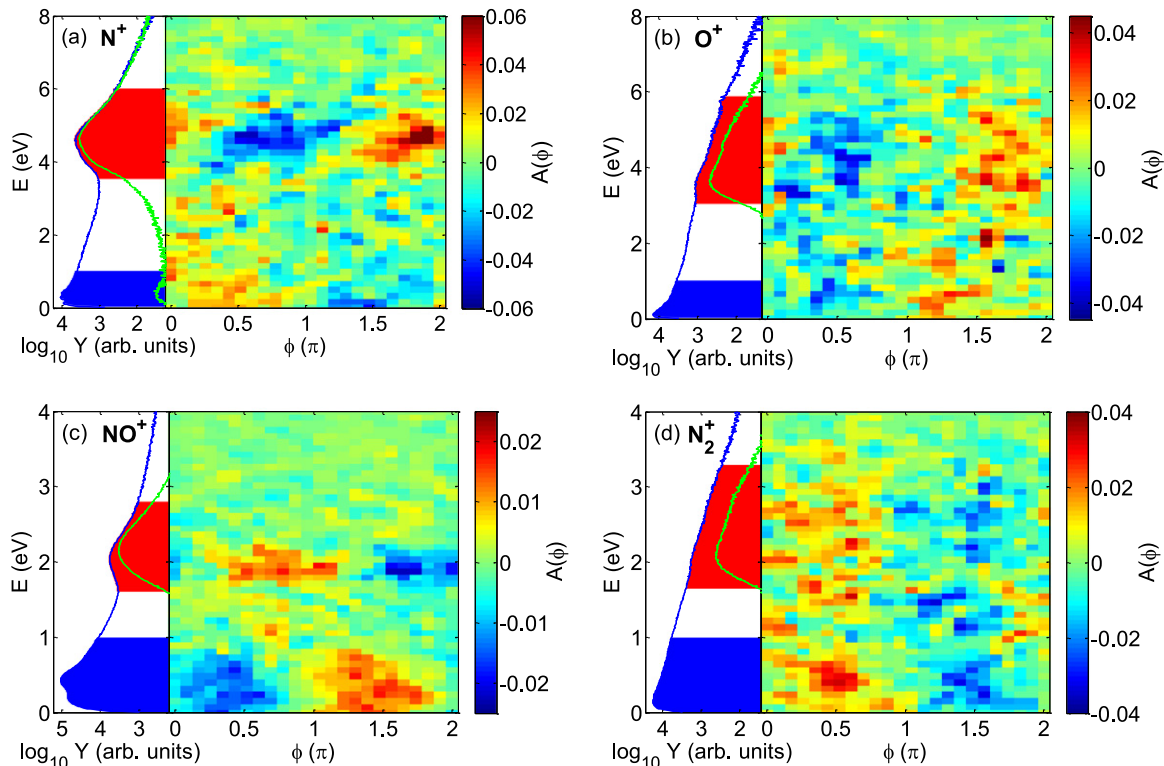
Figure 4. Asymmetry maps for various ionic fragments from the dissociative ionization of N_2O. Shown are the left–right asymmetries in the fragment yields along the laser polarization axis as a function of the fragments' energy and the CEP. The side panels display the kinetic energy spectra for each ion without coincidence filtering (blue line). The green lines are derived from the coincidences $N^+ + NO^+$, and $O^+ + N_2^+$ and are scaled with the estimated coincidence detection probability for all ion species. In each graph, low-energy and high-energy channels can be distinguished, as indicated by the corresponding blue and red colored areas of the energy spectra. The yields Y are given in the same units for each ion.

Table 1. Amplitudes A_0 and phase offsets ϕ_0 of the asymmetry oscillations for the low-energy and high-energy channels of each of the four ionic fragments without coincidence filtering. The offsets are given relative to the N_2O^+ recoil ion asymmetry for which $\phi_0 = 0$.

A_0	Low energy	High energy	ϕ_0	Low energy	High energy
N^+	$(2.5 \pm 0.2)\%$	$(3.7 \pm 0.2)\%$	N^+	$(8 \pm 7)°$	$(125 \pm 5)°$
NO^+	$(1.5 \pm 0.1)\%$	$(2.2 \pm 0.1)\%$	NO^+	$(194 \pm 2)°$	$(306 \pm 8)°$
O^+	$(1.5 \pm 0.1)\%$	$(3.8 \pm 0.3)\%$	O^+	$(191 \pm 9)°$	$(157 \pm 9)°$
N_2^+	$(1.6 \pm 0.1)\%$	$(2.6 \pm 0.2)\%$	N_2^+	$(354 \pm 7)°$	$(1 \pm 7)°$

suggests that the fragment asymmetries arise from the ionization step and are related to the geometry of the molecule. In principle, two scenarios can be invoked as a possible source for this behavior: either (i) the total probability for dissociative ionization is orientation dependent, which creates an oriented sample of molecular cations that dissociate; or (ii) the

probabilities for breaking either one of the two bonds depend differently on the CEP. The fact that the ions (N^+, N_2^+) and (O^+, NO^+), respectively, oscillate in phase clearly supports the first scenario. Similar observations have been made and conclusions have been drawn for asymmetries found in the dissociative ionization of CO [38, 40] and DCl [41].

The phase shift of approximately 120° between the high-energy and low-energy channels of N^+ and NO^+ corresponds to the offset between double and single ionization of N_2O (compare figure 3). The phase shift of 180° between the high-energy channels of N^+ and NO^+ already indicates that the majority of these fragments are the dissociation partners in the denitrogenation channel, which is further confirmed by the nearly identical amplitudes of the spectra of figure 4 in the high-energy ranges with and without a coincidence filter. Thus, the high-energy N^+ fragments follow the direction of motion of the dication while the fast NO^+ fragments are opposing it. This observation suggests that not only the initial ionization of the neutral molecule but also the probability for double ionization involving electron recollision is orientation dependent. If the second ionization were to be insensitive to the molecular orientation, the CEP value for zero asymmetry would be expected to be identical for the low-energy and high-energy channels, corresponding (predominantly) to the dissociation of the cation and dication. Since instead a phase shift between the channels is observed, we conclude that the recollision-induced ionization is orientation dependent.

In the case of O^+ and N_2^+ the phase shift between low-energy and high-energy channels is different from $120°$, which would indicate that the above argument is not applicable. However, as seen in figure 4, the high-energy channels of these two fragments contain significant numbers of non-coincident ions, which originate from the dissociation of the cation. In the case of N_2^+, whose high-energy channel is dominated by non-coincident ions, the low-energy and high-energy channels exhibit the same phase in the asymmetry oscillation. An analysis of the asymmetry of the coincident fragments from the dissociation of the dication is given in section 5.

Without coincidence filtering, contamination of the data with ions resulting from the ionization of background gas might play a role. In principle, N_2^+ ions can also originate from the ionization of residual N_2 in the REMI. However, these ions would neither have energies in the eV range nor exhibit the observed CEP dependence, because the recoil momenta from ionization alone are very small (up to 2.5 a.u.; cf figure 3(a)). The dissociative ionization of N_2 could also generate N^+ ions. These would be restricted to low energies, however, because no coincident $N^+ + N^+$ dissociation is observed in the PIPICO spectrum (figure 2). From the detected yield of low-energy N_2^+, we conclude that the dissociative ionization of N_2 is not a significant source of N^+ under the present experimental conditions. The same argument applies to the generation of O^+ from residual O_2 in the REMI. In principle, dissociation of H_2O^+ can also lead to the generation of O^+. This reaction, however, has been found to have a negligible quantum yield [66] and is therefore ruled out.

5. Coincident fragmentation channels

When analyzing the non-coincident channels, it is found that the N–N bond is 3.5 times more likely to break than the N–O bond. This yield ratio is, however, likely dominated by the
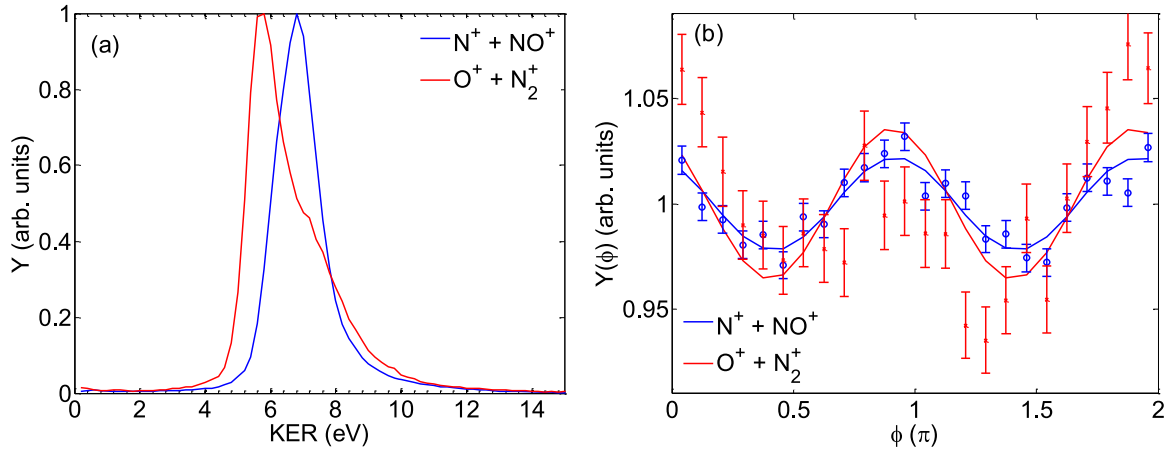
Figure 5. (a) Kinetic energy release (KER) spectra for the deoxygenation and denitrogenation of the N_2O dication induced by linearly polarized pulses with an intensity of 1.5×10^{14} W cm^{-2}. The maxima of both curves are normalized to 1. (b) CEP dependence of the yields of both channels normalized to their CEP-averaged yield. The error bars are of statistical nature and correspond to a standard deviation. The solid lines represent sinusoidal fit functions. The maxima in the coincident CEP-dependent fragmentation yields agree with the positions of the maxima for the high-energy, non-coincident N^+ and NO^+ fragments.

dissociation of the N_2O cation. In the coincident channels, with the generation of a momentum matched pair of ions, this trend is even more pronounced. For the conditions of our experiment, the denitrogenation yield is 6.2 times higher than the deoxygenation yield. At about twice the intensity, the ratio slightly increases to 6.7. For circular polarization (CP) a ratio of 13 is observed (clearly favoring the denitrogenation in circular polarization as compared to deoxygenation).

As seen in figure 5(a), the kinetic energy release (KER) spectrum of the deoxygenation channel is significantly broader than the one for the denitrogenation. It features a peak around 5.8 eV and a pronounced shoulder at 7.2 eV, whereas the denitrogenation channel has a narrow distribution round 6.8 eV. The KER spectra can be compared with earlier studies [33, 67] and allow for identifying contributing states in the dication. According to the potentials shown in figure 1 [50], the spectra can be explained by dissociation via the $3\Sigma^-$ and 3Π states of the N_2O dication. The following expected KER values can be read off from the diagram: for the dissociation reaction $N_2O^{2+} \rightarrow N_2^+ + O^+$, the expected KER values are approximately 5.8 eV for dissociation via the $3\Sigma^-$ state and 7.0 eV for dissociation via the 3Π state, while they are 6.8 eV and 11.4 eV, respectively, for the denitrogenation. However, Taylor *et al* reported that the 3Π state dissociates in the N–N stretching direction via fluorescent decay to the $3\Sigma^-$ state, resulting in the same KER [50]. This scheme agrees with our observation of a single peak in the KER spectrum. Despite the significantly lower deoxygenation yield in CP fields, we measure a slightly narrower KER distribution. Hence, electron recollision is particularly important in populating the higher excited states which lead to the ejection of an oxygen ion with high KER.

Figure 5(b) shows that both coincident dissociation channels exhibit a clear CEP-dependent modulation of their yields. Similar to our observation for the dication asymmetry, the modulation is stronger for deoxygenation. This agrees with the interpretation suggested in
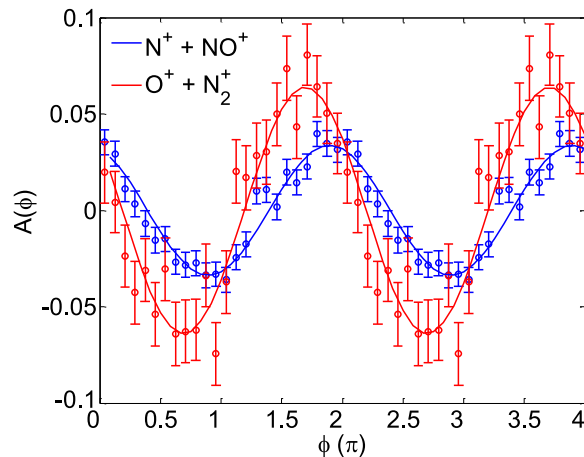
Figure 6. Comparison of the asymmetries for N^+ (blue) and O^+ (red) fragments detected in coincidence with momentum matched NO^+ and N_2^+ ions, respectively. A phase shift between the two channels of $(37 \pm 7)°$ is found by fitting sinusoidal functions with a period of 2π to the two curves (solid lines).

section 3 that the initiation of the deoxygenation reaction requires higher excitation energy as compared to denitrogenation. Analogously to the asymmetries of the momentum sums (figure 3(b)), the two yield curves are in phase with each other. A similar observation has been made for C_2H_2 and other hydrocarbons [43], where the CEP-dependent yields of various fragmentation channels were also in phase. The common phase offset of the yield modulations measured here is 120° and coincides with the phase offset of the dication asymmetry prior to dissociation.

A direct comparison of the asymmetries for the coincident fragmentation channels is given in figure 6. As for the yields, the CEP dependence of the asymmetry is stronger for the deoxygenation. The asymmetry in the N^+ yield from the denitrogenation channel oscillates in phase with the dication asymmetry prior to dissociation (cf figure 3), while the asymmetry in the O^+ yield from the deoxygenation channel exhibits a phase shift of $\Delta\phi = (37 \pm 7)°$ with respect to the dication asymmetry. Despite the limited statistics for the CEP dependence of the yield modulations shown in figure 5(b), it appears that the yield maxima coincide with the asymmetry extremes for the denitrogenation channels, while this is not the case for the deoxygenation channel.

The observation that the denitrogenation asymmetry shows the same phase offset as the dication asymmetry suggests that the denitrogenation asymmetry is caused by the orientation-dependent double-ionization process. According to this mechanism, the asymmetry in the O^+ yield from the deoxygenation pathway would be expected to exhibit a 180° phase shift with respect to the dication asymmetry. However, the dissociation step in the deoxygenation appears to be influenced by the laser, resulting in the phase shift $\Delta\phi$.

As shown in figure 7 and in accord with the results of a synchrotron experiment [68], we observe very similar angular distributions for the two pathways. However, we measure a deeper dip in the deoxygenation yield perpendicular to the polarization, $\theta \approx 90°$, as shown in figure 7(a). This difference may arise from a small contribution of the decay of metastable states to the denitrogenation yield [50], such as the 3Π state, which dissociates on a time scale
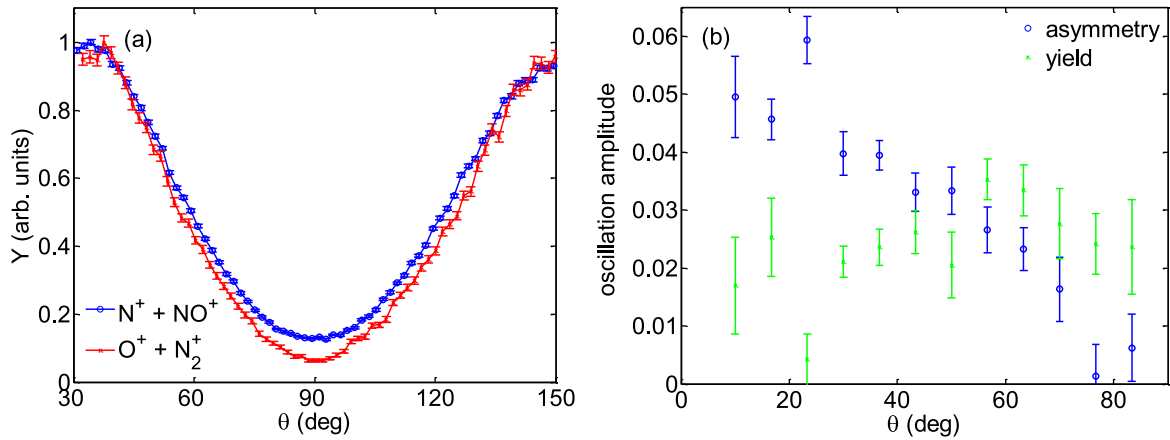
Figure 7. (a) Differential yield of coincident ion pairs from deoxygenation (red crosses) and denitrogenation (blue circles) of N_2O per unit solid angle as a function of the polar angle θ, normalized to their respective maxima. In the angular ranges $[0°, 30°]$ and $[150°, 180°]$, quantitative analysis is hampered by inhomogeneous detection efficiency in the experiment and thus not performed. (b) Amplitudes of the 2π-periodic asymmetry (blue) and π-periodic total-yield modulations (green) as a function of the polar angle for the denitrogenation channel. The data for each point are integrated over the azimuthal angle ϕ.

comparable to or longer than the N_2O rotational period of 39.77 ps [69]. Hence, this process would smear out the angular distribution. Note that the observed phase shift $\Delta\phi$ (see figure 6) between the two dissociation pathways is insensitive to the chosen angular integration range.

In figure 7(b), we present the asymmetry and yield modulation amplitude for the denitrogenation channel as functions of the CEP and polar angle θ. The asymmetry amplitude clearly decreases with increasing polar angle and vanishes at $90°$ as expected for geometrical reasons. The yield modulation, however, is observed to be essentially isotropic. We may attempt to compare our results to the ones from the two-color experiment of Kotsina *et al* [52], who analyzed the phase dependences of the forward and backward denitrogenation yields separately. Generally, one can expect a phase-dependent modulation of the total yield with period π and left–right asymmetry modulation with period 2π. Therefore, an analysis of either the forward or backward yield would result in a superposition of two sinusoidal forms with periodicities of π and 2π. Because of the different angular dependences of the asymmetry and yield modulations (see figure 7(b)), different CEP-dependent oscillation behaviors are expected for different polar angles. Due to the vanishing asymmetry at $90°$, the yield modulation is the only contribution. Furthermore, in our data the asymmetry modulation dominates at small θ. An angle-dependent variation in the directional yield modulation was also reported by Kotsina *et al* [52]. While these authors made contributions from two channels responsible for this behavior, we propose an alternative explanation based solely on the angle dependence of the asymmetry and yield modulation. For completeness, we also analyzed the dependence of the asymmetry and yield amplitudes for the deoxygenation channel, but found no clear trends for the present experimental conditions.

6. Summary and outlook

We have studied CEP effects in the total and directional fragment yields in the strong-field dissociative ionization of N_2O by 4 fs laser pulses. Using phase-tagged ion–ion coincidence momentum imaging allows us to distinguish between asymmetries acquired in the ionization and the dissociation steps. The CEP-dependent dication recoil momentum spectra, obtained from the momentum sum of the coincident ions, demonstrate that electron recollision is the dominant route to double ionization for the present laser conditions. The observed characteristic phase shifts in the asymmetries of directional ion emissions allow for comparison of contributions from single ionization by the laser field, recollision-induced double ionization and dissociation of the molecular ions.

In particular, these phase shifts allow us to establish that the laser creates oriented samples of molecular ions which undergo dissociation. We find that not only the field ionization but also the electron-recollision-induced double ionization of N_2O is orientation dependent. The selection of oriented molecules in both ionization steps can explain all observations for the denitrogenation channel. The origin of the measured phase shift of 37° in the asymmetry of the deoxygenation channel, however, is not yet understood. Theoretical work, involving the laser-induced coupling of the electronic states of the dication involved may shed light on the origin of the phase shift.

Future kinematically complete studies, where the electrons from the double ionization of N_2O are also detected, would help with elucidating the multi-electron dynamics underlying the strong-field control.

References

[1] Baltuška A *et al* 2003 *Nature* **421** 611–5
[2] Goulielmakis E, Yakovlev V S, Cavalieri A L, Uiberacker M, Pervak V, Apolonski A, Kienberger R, Kleineberg U and Krausz F 2007 *Science* **317** 769–75
[3] Krausz F and Ivanov M 2009 *Rev. Mod. Phys.* **81** 163
[4] Cerullo G, Baltuška A, Mücke O and Vozzi C 2011 *Laser & Phot. Rev.* **5** 323–51
[5] Kling M F, von den Hoff P, Znakovskaya I and de Vivie-Riedle R 2013 *Phys. Chem. Chem. Phys.* **15** 9448–67
[6] Weinkauf R, Schanen P, Yang D, Soukara S and Schlag E W 1995 *J. Phys. Chem.* **99** 11255–65
[7] Znakovskaya I *et al* 2012 *Phys. Rev. Lett.* **108** 063002
[8] Lépine F, Sansone G and Vrakking M J J 2013 *Chem. Phys. Lett.* **578** 1–14

  [9] Bandrauk A D, Chelkowski S and Nguyen H S 2004 *Int. J. Quant. Chem.* **100** 834–44
 [10] Roudnev V, Esry B D and Ben-Itzhak I 2004 *Phys. Rev. Lett.* **93** 163601
 [11] Kling M F *et al* 2006 *Science* **312** 246–8
 [12] Gräfe S and Ivanov M Y 2007 *Phys. Rev. Lett.* **99** 163603
 [13] Tong X M and Lin C D 2007 *Phys. Rev. Lett.* **98** 123002
 [14] He F, Ruiz C and Becker A 2007 *Phys. Rev. Lett.* **99** 083002
 [15] Roudnev V and Esry B D 2007 *Phys. Rev.* A **76** 023403
 [16] Kling M F, Siedschlag C, Znakovskaya I, Verhoef A J, Zherebtsov S, Krausz F, Lezius M and Vrakking M J J 2008 *Mol. Phys.* **106** 455–65
 [17] He F, Becker A and Thumm U 2008 *Phys. Rev. Lett.* **101** 213002
 [18] Geppert D, von den Hoff P and de Vivie-Riedle R 2008 *J. Phys.* B **41** 074006
 [19] Kremer M *et al* 2009 *Phys. Rev. Lett.* **103** 213003
 [20] von den Hoff P, Znakovskaya I, Kling M F and de Vivie-Riedle R 2009 *Chem. Phys.* **366** 139–47
 [21] Fischer B, Kremer M, Pfeifer T, Feuerstein B, Sharma V, Thumm U, Schröter C D, Moshammer R and Ullrich J 2010 *Phys. Rev. Lett.* **105** 223001
 [22] Kelkensberg F, Sansone G, Ivanov M Y and Vrakking M 2011 *Phys. Chem. Chem. Phys.* **13** 8647–52
 [23] Anis F and Esry B D 2012 *Phys. Rev. Lett.* **109** 133001
 [24] Xu H, Maclean J P, Laban D E, Wallace W C, Kielpinski D, Sang R T and Litvinyuk I V 2013 *New J. Phys.* **15** 023034
 [25] Kling N G *et al* 2013 *Phys. Rev. Lett.* **111** 163004
 [26] Rathje T, Sayler A M, Zeng S, Wustelt P, Figger H, Esry B D and Paulus G G 2013 *Phys. Rev. Lett.* **111** 093002
 [27] Li H *et al* 2014 *J. Phys. B: At. Mol. Opt. Phys.* **47** 124020
 [28] Singh K P *et al* 2010 *Phys. Rev. Lett.* **104** 023001
 [29] Sansone G *et al* 2010 *Nature* **465** 763–6
 [30] Ranitovic P *et al* 2014 *Proc. Natl Acad. Sci. USA* **111** 912–7
 [31] Gagnon E, Ranitovic P, Tong X M, Cocke C L, Murnane M M, Kapteyn H C and Sandhu A S 2007 *Science* **317** 1374–8
 [32] Sandhu A S, Gagnon E, Santra R, Sharma V, Li W, Ho P, Ranitovic P, Cocke C L, Murnane M M and Kapteyn H C 2008 *Science* **322** 1081–5
 [33] Zhou X, Ranitovic P, Hogle C W, Eland J H D, Kapteyn H C and Murnane M M 2011 *Nat. Phys.* **8** 232–7
 [34] Siu W *et al* 2011 *Phys. Rev.* A **84** 063412
 [35] Calegari F *et al* 2013 http://dx.doi.org/10.1364/CLEO_QELS.2013.QF2C.5
 [36] Neidel C 2013 *Phys. Rev. Lett.* **111** 033001
 [37] Kübel M *et al* 2013 *Phys. Rev.* A **88** 023418
 [38] Znakovskaya I, von den Hoff P, Zherebtsov S, Wirth A, Herrwerth O, Vrakking M J J, de Vivie-Riedle R and Kling M F 2009 *Phys. Rev. Lett.* **103** 103002
 [39] Liu Y, Liu X, Deng Y, Wu C, Jiang H and Gong Q 2011 *Phys. Rev. Lett.* **106** 073004
 [40] Betsch K J *et al* 2012 *Phys. Rev.* A **86** 063403
 [41] Znakovskaya I, von den Hoff P, Schirmel N, Urbasch G, Zherebtsov S, Bergues B, de Vivie-Riedle R, Weitzel K M and Kling M F 2011 *Phys. Chem. Chem. Phys.* **13** 8653–8
 [42] Bayer T, Braun H, Sarpe C, Siemering R, von den Hoff P, de Vivie-Riedle R, Baumert T and Wollenhaupt M 2013 *Phys. Rev. Lett.* **110** 123003
 [43] Xie X *et al* 2012 *Phys. Rev. Lett.* **109** 243001
 [44] Mathur D, Dota K, Dharmadhikari A K and Dharmadhikari J A 2013 *Phys. Rev. Lett.* **110** 083602
 [45] Barth I, Manz J, Shigeta Y and Yagi K 2006 *J. Am. Chem. Soc.* **128** 7043–9
 [46] von den Hoff P, Siemering R, Kowalewski M and de Vivie-Riedle R 2011 *IEEE J. Sel. Top. Quant. Electron* **18** 119–29
 [47] Lötstedt E and Midorikawa K 2013 *Phys. Rev.* A **88** 041402(R)

[48] Miura S *et al* 2014 *Chem. Phys. Lett.* **595–596** 61–6 (http://www.sciencedirect.com/science/article/pii/S0009261414000542)

[49] Alnaser A S *et al* 2014 *Nat. Commun.* **5** 3800 (http://www.nature.com/ncomms/2014/140508/ncomms4800/full/ncomms4800.html)

[50] Taylor S, Eland J H D and Hochlaf M 2006 *J. Chem. Phys.* **124** 204319

[51] Alagia M, Candori P, Falcinelli S, Lavollée M, Pirani F, Richter R, Stranges S and Vecchiocattivi F 2006 *Chem. Phys. Lett.* **432** 398–402

[52] Kotsina N, Kaziannis S, Danakas S and Kosmidis C 2013 *J. Chem. Phys.* **139** 104313

[53] Brumer P and Shapiro M 1986 *Chem. Phys. Lett.* **126** 541–6

[54] Shapiro M and Brumer P 1986 *J. Chem. Phys.* **84** 4103–4

[55] Shapiro M, Hepburn J W and Brumer P 1988 *Chem. Phys. Lett.* **149** 451–4

[56] Shapiro M and Brumer P 2000 *Adv. At. Mol. Opt. Phys.* **42** 287–345

[57] Abel M, Neumark D M, Leone S R and Pfeifer T 2011 *Laser & Phot. Rev.* **5** 352–67

[58] Bergues B *et al* 2012 *Nat. Commun.* **3** 813

[59] Johnson N G *et al* 2011 *Phys. Rev.* A **83** 013412

[60] Wittmann T, Horvath B, Helml W, Schätzel M G, Gu X, Cavalieri A L, Paulus G G and Kienberger R 2009 *Nat. Phys.* **5** 357–62

[61] Rathje T, Johnson N G, Möller M, Süßmann F, Adolph D, Kübel M, Kienberger R, Kling M F, Paulus G G and Sayler A M 2012 *J. Phys.* B **45** 074003

[62] Ullrich J, Moshammer R, Dorn A, Dörner R, Schmidt L P H and Schmidt-Böcking H 2003 *Rep. Prog. Phys.* **66** 1463

[63] Field T A and Eland J H D 1993 *Chem. Phys. Lett.* **211** 436–42

[64] Hsieh S and Eland J 1997 *J. Phys.* B **30** 452–34

[65] Tong X M and Lin C D 2005 *J. Phys. B: At. Mol. Opt. Phys.* **38** 2593

[66] Sage A G, Oliver T A A, Dixon R N and Ashfold M N R 2010 *Mol. Phys.* **108** 945–55

[67] Price S D, Eland J H D, Fournier P G, Fournier J and Millie P 1988 *J. Chem. Phys.* **88** 211–5

[68] Alagia M, Candori P, Falcinelli S, Lavollée M, Pirani F, Richter R, Stranges S and Vecchiocattivi F 2007 *J. Chem. Phys.* **126** 201101

[69] Zeng G, Wu C, Jiang H, Gao Y, Xu N and Gong Q 2009 *J. Phys. B: At. Mol. Opt. Phys.* **42** 165508